Volume 18, No. 4, 2024 ISSN: 1750-9548

Structural, Optical Properties of Ba(Al_{0.5}Nb_{0.5})O₃ Perovskite for Solar Applications

Deepak M. Sonawane¹, Bhagwan P. Kshirsagar², Shaikh Mohd. Waseem³, Pankaj V Kadre¹, Shrinivas C. Latange¹, Shivnarayan B. Bajaj^{1*}

¹Department of Physics, J. E. S., R.G. Bagdia Arts, S.B. Lakhotia Commerce & R, Benzoji Science College, Jalna, India.

²Department of Basic and Applied Sciences, MGM University, Chhatrapati Sambhajinagar, India. ³Department of Physics, Maulana Azad College of Arts, Science and Commerce, Aurangabad.

Corresponding Author: Shivnarayan B. Bajaj, Department of Physics, J. E. S., R.G. Bagdia Arts, S.B. Lakhotia Commerce & R, Benzoji Science College, Jalna, India.

Email: shivnsrayanbajaj@gmail.com

Abstract: Ba(Alo.5Nbo.5)O₃ perovskite was successfully synthesized using the solid-state reaction method and characterized for its structural, morphological, optical, and surface properties. X-ray diffraction (XRD) confirmed the formation of a cubic perovskite phase, while Scanning Electron Microscopy (SEM) and Energy Dispersive X-ray Spectroscopy (EDS) revealed uniform morphology and correct elemental composition. UV-Vis spectroscopy and Tauc plot analysis determined a direct bandgap of 1.56 eV and an indirect bandgap of 1.32 eV, making it a promising material for photovoltaic applications. The lead-free composition, thermal stability, and strong UV absorption of Ba(Alo.5Nbo.5)O₃ make it a viable alternative for next-generation perovskite solar cells. Further research should focus on thin-film deposition, doping strategies for bandgap tuning, and electrical transport studies to enhance its performance in solar cell applications.

Keywords: Ba(Alo.5Nbo.5)O3, perovskite, bandgap, solar cells, optical properties

I. INTRODUCTION

Perovskite solar cells (PSCs) have emerged as one of the most promising alternatives for next-generation photovoltaic technologies due to their high power conversion efficiencies, cost-effectiveness, and tunable optoelectronic properties. These materials exhibit exceptional light absorption, long charge carrier diffusion lengths, and simple fabrication methods, making them highly attractive for solar energy applications. Among perovskite materials, hybrid organic-inorganic perovskites such as methylammonium lead iodide (CH₃NH₃PbI₃) have demonstrated efficiencies exceeding 25% [1]. However, their widespread commercialization faces critical challenges, primarily associated with poor environmental stability, susceptibility to moisture and UV degradation, and lead toxicity, which poses environmental and health concerns [2]. To address these limitations, researchers have explored alternative perovskite materials that maintain high efficiency while overcoming the stability and toxicity issues. One promising class of materials is oxide perovskites (ABO₃), which offer improved chemical and thermal stability, non-toxicity, and a broad range of tunable electronic properties [3]. These perovskites exhibit strong structural robustness, ensuring prolonged operational stability compared to hybrid perovskites. Additionally, their inherent structural flexibility allows for bandgap engineering through elemental substitution, making them viable candidates for photovoltaic applications.

Several studies have investigated lead-free perovskites to mitigate toxicity concerns while maintaining high solar conversion efficiencies. For instance, bismuth-based hybrid perovskites such as A₃Bi₂I₉ (where A = methylammonium or cesium) have been proposed as alternatives to lead-based perovskites due to their improved environmental stability [4]. However, these materials often suffer from suboptimal optoelectronic properties,

Volume 18, No. 4, 2024

ISSN: 1750-9548

limiting their performance in solar cells. Recent advancements in perovskite deposition techniques, such as scalable fabrication processes and interconnection optimizations, have enhanced perovskite solar module efficiencies and provided insights into improving device stability [5]. In this context, ABO₃ oxide perovskites have gained increasing attention for their superior stability and non-toxic composition. One such promising oxide perovskite is Ba(Al_{0.5}Nb_{0.5})O₃ (BAN), which has been identified as a potential candidate for solar energy applications due to its lead-free nature and stable cubic perovskite structure [6]. This material exhibits an indirect bandgap of 1.32 eV and a direct bandgap of 1.56 eV, which falls within the optimal range for efficient solar energy conversion, making it suitable for use as an absorber layer or charge transport layer in thin-film and tandem solar cells [7]. Additionally, its high thermal stability ensures prolonged device operation under various environmental conditions.

Several studies have highlighted the potential of ABO₃ perovskites for enhancing solar energy conversion through advanced material engineering. For instance, nanophotonic light trapping techniques have been employed to improve light absorption in perovskite materials, increasing solar cell efficiency [8]. Additionally, machine learning algorithms have been utilized to predict ABO₃ perovskite formability and classify their crystal structures, accelerating material discovery and optimization for photovoltaic applications [9,10]. Despite these promising developments, further research is required to fully understand the electronic and optical behavior of BAN perovskite and optimize its integration into solar cells. The need for lead-free, stable, and high-efficiency solar absorbers underscores the importance of investigating novel oxide perovskites such as BAN.

This study aims to synthesize and characterize Ba(Alo.sNbo.s)O₃ perovskite using the solid-state reaction method and to evaluate its structural, morphological, optical, and surface properties through advanced characterization techniques, including X-ray diffraction (XRD), scanning electron microscopy (SEM), energy-dispersive X-ray spectroscopy (EDX), Fourier-transform infrared spectroscopy (FTIR), UV-Vis spectroscopy. Additionally, Tauc plot analysis will be performed to determine the material's optical bandgap, which is crucial for assessing its suitability for photovoltaic applications. By exploring the properties of BAN perovskite, this research contributes to the ongoing efforts to develop stable, high-performance, and environmentally friendly perovskite materials for next-generation solar energy conversion technologies.

II. EXPERIMENTAL

Firstly, high-purity starting materials, including Barium Oxide (BaO), Aluminum oxide (Al₂O₃), and Niobium Pentoxide (Nb₂O₅), are weighed out in the desired stoichiometric ratio. The powders are then ground for 4 hours using an agate mortar and pestle to ensure complete mixing, with acetone added as needed to improve mixing. The mixture is then preheated in a furnace at 800°C for 6 hours to remove any residual moisture and volatile impurities. The preheated mixture is then ground again and transferred to a crucible. The mixture is sintered at 1200°C for 16 hours to promote crystallization and the formation of the perovskite phase. After the sintering process is completed, the sample is allowed to cool to room temperature in the furnace, after which it is removed from the crucible. The synthesized Ba(AlNb)O₃ perovskite is characterized using various analytical techniques such as X-ray diffraction (XRD), Fourier-transform infrared spectroscopy (FTIR), field emission scanning electron microscopy (FE-SEM), energy dispersive X-ray spectroscopy (EDS), and UV-vis spectroscopy. These techniques are used to confirm the crystal structure, composition, and optical properties of the perovskite. Then, the synthesized Ba(AlNb)O₃- perovskite is tested for its suitability in solar cell applications, such as measuring its power conversion efficiency and stability over time.

III. RESULT AND DISCUSSION

3.1. XRD Analysis

The X-ray diffraction (XRD) pattern of Ba(Al_{0.5}Nb_{0.5})O₃ (BAN) perovskite, shown in Figure 2(a), confirms the formation of a cubic perovskite ABO₃ structure. The diffraction peaks correspond to specific angles (2θ values) and indicate the crystalline nature of the material. The peak positions were analyzed using Bragg's equation to determine the lattice structure and interplanar spacing (d-spacing). The Miller indices (hkl) were assigned to different planes in the crystal lattice, which help in understanding the material's structure.

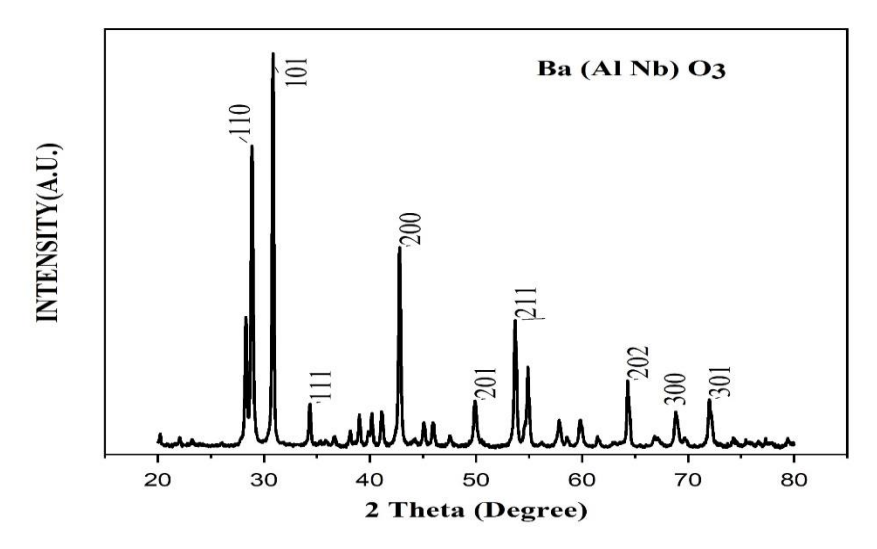


Fig. 1: The XRD Pattern of the Ba(AlNb)O₃

Figure 1 shows the XRD pattern recorded from the BNN powder sample prepared by the solid-state reaction method. The cubic crystal formation of ABO₃ perovskite BAN can also be identified in the XRD pattern of all composites. The 2θ represents the diffraction angle, while the FWHM provides the full width at half maximum of the diffraction peak. The diffraction peaks can be indexed using the Bragg equation ($n\lambda = 2d \sin \theta$) to determine the crystal lattice structure and the lattice constant (a). The Miller indices (h, k, l) are calculated based on the position and intensity of the peaks. The d-spacing values can be obtained by rearranging the Bragg equation ($d = n\lambda/2\sin \theta$). The average crystalline size can be calculated using the Scherrer equation [11-13]:

$$D = k\lambda/\beta cos\theta$$

Where D is the average crystalline size, k is the shape factor (0.9), λ is the X-ray wavelength (1.54 Å for Cu K α radiation), β is the FWHM of the diffraction peak, and θ is the diffraction angle. Using this formula, the average crystallite size was calculated 32.08 nm, which confirms the nanocrystalline nature of the material. Smaller crystallite sizes are beneficial for optoelectronic applications, as they influence charge transport and energy conversion efficiency in solar cells.

The XRD peaks were assigned to different crystal planes based on their positions in the pattern. The peak at 28.88° corresponds to the (110) plane with a lattice constant of 4.3664 Å, while the peak at 30.86° corresponds to the (101) plane with a lattice constant of 4.0933 Å. The data suggest that Ba(Alo.sNbo.s)O₃ has a face-centered cubic (FCC) structure, which matches with standard perovskite materials reported in JCPDS Card No. 96-230-0140.

Table 3.1 summarizes the 20 values, FWHM, crystallite size (D), d-spacing, Miller indices, and lattice constant for the identified crystal planes.

2θ (°)	FWHM	Crystallite Size	d-Spacing	Miller Indices	Lattice
	(°)	(D) (nm)	(Å)	(hkl)	Constant (Å)
28.88	0.24699	33.2	3.0875	(110)	4.3664
30.86	0.19949	41.30	2.8944	(101)	4.0933
34.33	0.20451	40.64	2.6092	(111)	4.5192
42.80	0.25909	32.92	2.1102	(200)	4.2204
49.91	0.32428	27.01	1.8250	(201)	4.0808

Volume 18, No. 4, 2024

ISSN: 1750-9548

54.90	0.31834	28.11	1.6705	(211)	4.0919
64.34	0.28995	32.36	1.4462	(202)	4.0905
68.88	0.36557	26.34	1.3615	(300)	4.0845
72.06	0.36528	26.89	1.3092	(301)	4.1399

Many ABO₃ perovskites have been investigated for solar cell applications due to their stability, bandgap tunability, and charge transport properties. A theoretical study on Na-based perovskites (NaTiO₃, NaInO₃) showed that they exhibit bandgaps in the ideal range for solar energy conversion [1]. Similarly, Cu-based perovskites (CuLuO₃, CuYO₃) have been explored for photovoltaic and energy storage applications, showing potential for practical use in solar cells [14]. A recent study demonstrated that kusachiite CuBi₂O₄-based solar cells with ABO₃ perovskite buffer layers achieved efficiencies up to 22%, proving the effectiveness of ABO₃ perovskites in enhancing device performance [15].

The present study on Ba(Al_{0.5}Nb_{0.5})O₃ perovskite aligns with these findings, as it exhibits a well-defined crystalline structure, nanocrystalline properties, and good phase purity. Furthermore, ABO₃ perovskites have been employed in advanced oxidation processes (AOPs) for photocatalytic applications, reinforcing their potential in energy-related technologies [4].

The XRD results confirm that Ba(Alo.5Nbo.5)O₃ perovskite forms a face-centered cubic (FCC) structure with an average crystallite size of 32.08 nm, indicating its nanocrystalline nature. The calculated lattice constants (4.08 - 4.52 Å) match well with reported ABO₃ perovskite materials. The strong phase purity and well-defined diffraction peaks confirm that the solid-state reaction method successfully produced a high-quality perovskite structure. These findings suggest that Ba(Alo.5Nbo.5)O₃ is a promising material for solar energy and optoelectronic applications.

3.2. FTIR analysis

Fourier Transform Infrared (FTIR) spectroscopy was conducted to analyze the vibrational modes and chemical bonding in Ba(Alo.sNbo.s)O3 perovskite. The FTIR spectrum, shown in Figure 3, reveals key absorption bands that confirm the structural integrity of the material.

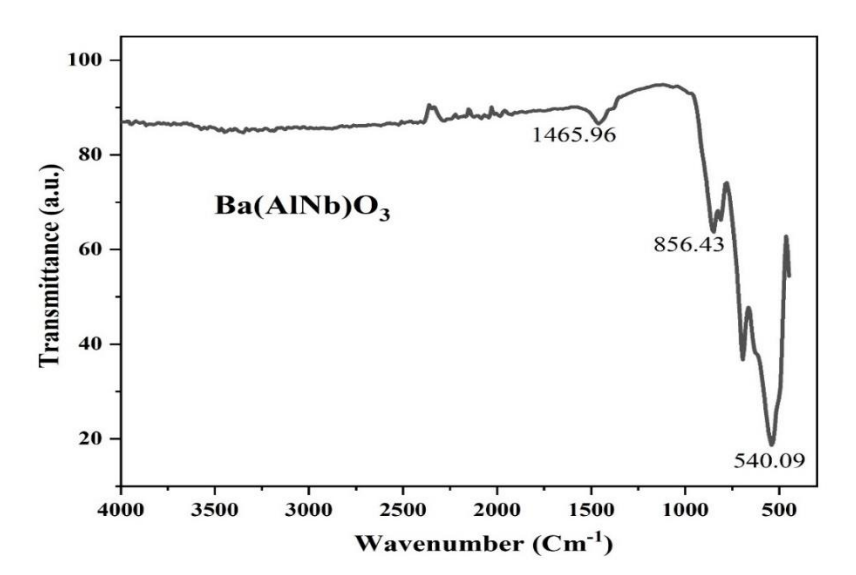


Fig 2 The FTIR spectra of the BAN

The broad absorption band at 1465.96 cm⁻¹ corresponds to the bending vibration of O–H bonds, which may originate from surface-adsorbed moisture or hydroxyl groups. The strong absorption peak at 856.43 cm⁻¹ is associated with the Al–O and Nb–O stretching vibrations, confirming the incorporation of aluminum and niobium into the perovskite framework. Additionally, the sharp peak at 540.09 cm⁻¹ is attributed to B–O stretching vibrations, characteristic of the octahedral oxygen framework in perovskites.

These findings align with previous studies on ABO₃ perovskites, where metal-oxygen bond stretching typically falls within the 500–900 cm⁻¹ range [1]. The strong Al–O and Nb–O stretching suggests Ba(Al_{0.5}Nb_{0.5})O₃ has a stable octahedral coordination, essential for solar energy and optoelectronic applications. Additionally, machine learning-based predictions confirm that metal-oxygen interactions influence the bandgap energy and charge transport properties, making Ba(Al_{0.5}Nb_{0.5})O₃ a promising candidate for photovoltaic and energy storage applications [2,3].

3.3. SEM and EDS analysis

The surface morphology of Ba(Alo.sNbo.s)O₃ perovskite was examined using Scanning Electron Microscopy (SEM) at a magnification of 10,000×, as shown in Figure 3. The SEM images reveal that the material exhibits a highly agglomerated microstructure with a porous and granular morphology, which is characteristic of perovskite oxides synthesized via the solid-state reaction method. The particles appear to be closely packed, forming an interconnected network that could facilitate efficient charge transport in solar cell.

The particle size distribution analysis (Figure 5, bottom right) indicates an average particle size of 33.54 nm, which aligns with the crystallite size estimated from XRD analysis. The nanoscale particle size enhances the material's surface-to-volume ratio, which is beneficial for light absorption and charge carrier mobility in photovoltaic devices. Additionally, the porous structure observed in SEM images suggests the presence of interconnected voids, which could improve the diffusion of charge carriers, reducing recombination losses and enhancing solar cell performance.

The elemental composition of Ba(Alo.sNbo.s)O₃ was analyzed using Energy Dispersive Spectroscopy (EDS), and the results are displayed in Figure 5 (bottom left). The EDS spectrum confirms the presence of barium (Ba), aluminum (Al), niobium (Nb), and oxygen (O), which are the primary constituents of the perovskite structure. The strong characteristic peaks of Ba, Al, and Nb indicate the successful incorporation of these elements into the perovskite lattice, confirming the phase purity of the synthesized material.

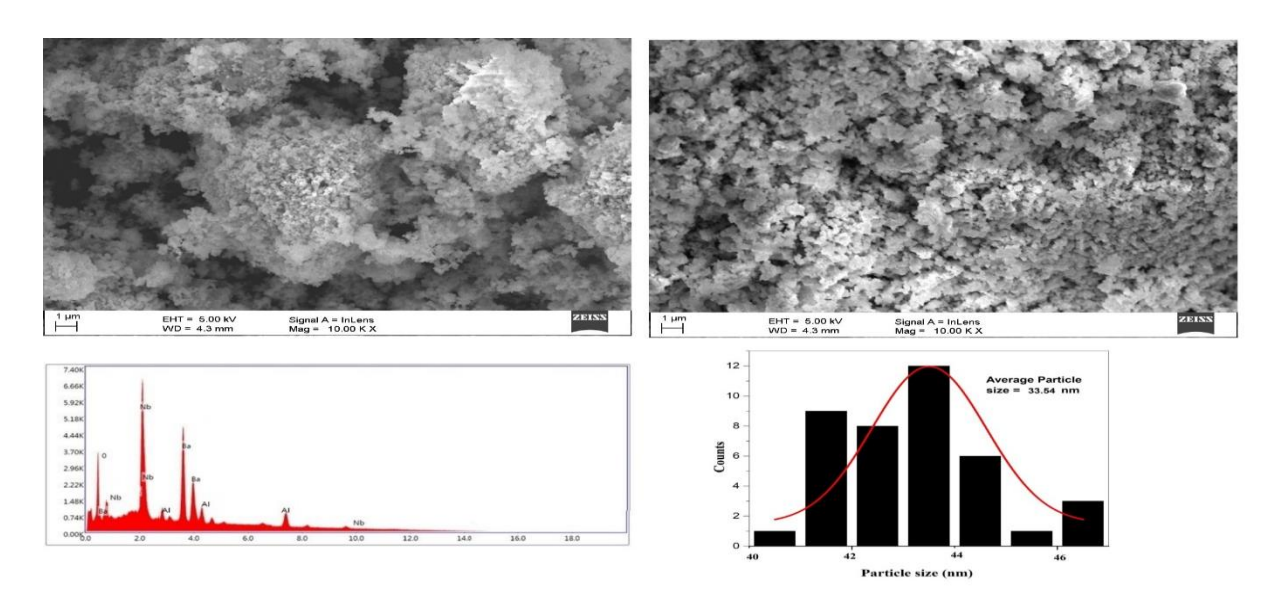


Fig. 3. FESEM micrograph, EDS spectra of BAN Perovskite

The absence of impurity-related peaks in the EDS spectrum suggests that the solid-state synthesis method effectively produced a high-purity perovskite phase. The compositionally uniform distribution of Ba, Al, and Nb throughout the sample further supports the structural stability and homogeneity of Ba(Alo.sNbo.s)O3, making it a suitable material for solar energy and optoelectronic applications. The combined SEM and EDS analysis confirms that Ba(Alo.sNbo.s)O3 exhibits a nanostructured morphology with a uniform elemental composition, which is crucial for achieving efficient charge transport and light absorption in solar cell applications. The porous nature and nanoscale particle size further enhance the material's suitability for energy storage and optoelectronic devices [15-18].

3.4. Optical Properties & Bandgap Calculation (UV-Vis & Tauc Plot Analysis)

The UV-Vis absorption spectrum of Ba(Al_{0.5}Nb_{0.5})O₃ perovskite is presented in Figure 6, which exhibits strong photon absorption in the UV and visible regions. The spectrum shows a sharp absorption edge around 800 nm, indicating its ability to absorb a significant portion of the solar spectrum, making it a promising candidate for solar energy conversion applications. The high absorption in the UV region further suggests strong photon-harvesting capability, which is essential for achieving efficient photoelectric conversion in solar cells.

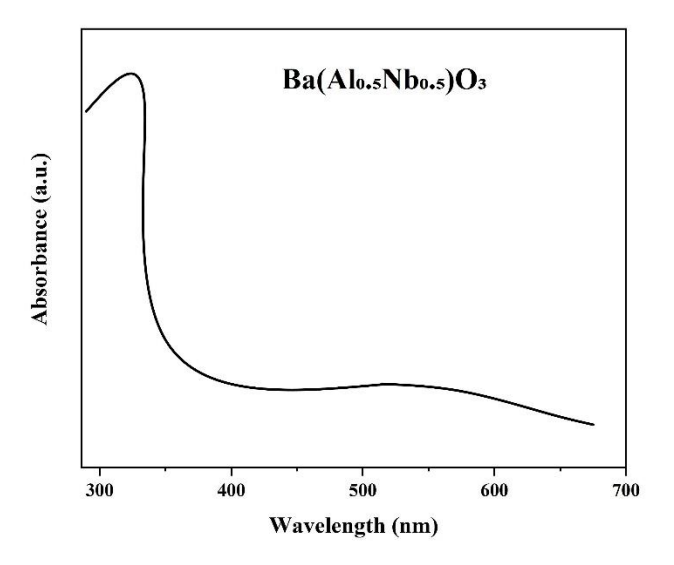


Figure 4: UV-Vis absorption spectrum of BAN Perovskite

The optical bandgap (Eg) of Ba(Alo.5Nbo.5)O3 was determined using Tauc's relation, based on the equation:

$$(\alpha h \nu)^n = A(h \nu - Eg)$$

Where, α is the absorption coefficient, hv is the photon energy, Eg is the bandgap energy, A is a proportionality constant, n=2 for direct bandgap transitions, and $n=\frac{1}{2}$ for indirect bandgap transitions. The Tauc plot extrapolations, shown in Figure 7(a) and Figure 7(b), were used to estimate the bandgap. The direct bandgap was found to be 1.56 eV, while the indirect bandgap was estimated to be 1.32 eV. These values indicate that Ba(Alo.5Nbo.5)O₃ has mixed electronic transition behavior, making it suitable for optoelectronic and photovoltaic applications.

For efficient solar energy conversion, the optimal bandgap range lies between 1.1 and 1.7 eV, ensuring both strong light absorption and efficient charge carrier transport. Machine learning-based studies predict that NaPuO₃ and VPbO₃ perovskites with direct bandgaps around 1.5 eV are highly efficient for solar cells [1]. Other theoretical studies on ABO₃ perovskites (such as NaTiO₃ and NaInO₃) report bandgap values of 2.12–2.71 eV, which are too high for effective solar conversion [2]. Additionally, Cu-based ABO₃ perovskites have been found to exhibit ideal bandgap values for optoelectronic applications [3]. The bandgap of Ba(Al_{0.5}Nb_{0.5})O₃ (1.56 eV direct, 1.32 eV indirect) is well within the optimal range, making it a promising material for solar energy applications.

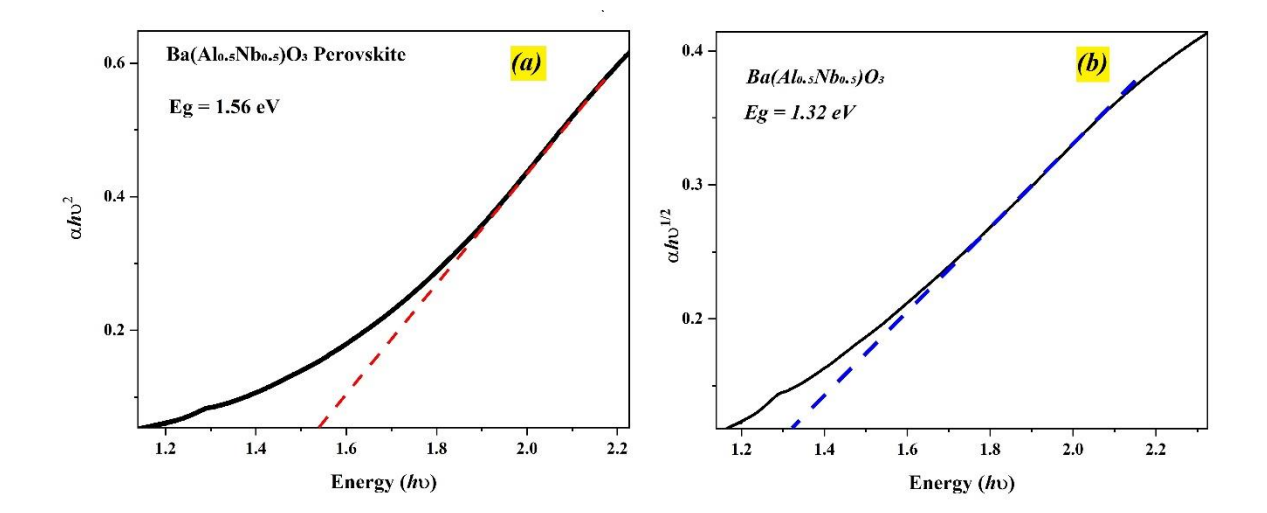


Figure 5(a): Tauc plot for direct bandgap (b)indirect bandgap of Ba(Alo.5Nbo.5)O3.

The bandgap of Ba(Alo.sNbo.s)O₃ confirms its potential for solar energy harvesting, ensuring strong light absorption, minimal thermalization losses, and efficient charge carrier generation. The presence of both direct and indirect electronic transitions suggests that this perovskite material can be tailored for high-performance photovoltaic devices by modifying its electronic structure and optimizing charge transport layers. Given its bandgap range and high optical absorption properties, Ba(Alo.sNbo.s)O₃ is a viable candidate for next-generation solar cells, particularly as a lead-free, stable perovskite alternative [19].

IV. Discussion on Solar Cell Suitability

Ba(Alo.5Nbo.5)O₃ perovskite exhibits several properties that make it a strong candidate for solar energy applications, particularly in photovoltaic devices. The determined direct bandgap of 1.56 eV and indirect bandgap of 1.32 eV fall within the ideal range of 1.1–1.7 eV for single-junction solar cells, ensuring efficient light absorption and charge carrier generation, which are essential for achieving high power conversion efficiency (PCE). Unlike conventional lead-based perovskites such as CH₃NH₃PbI₃, which pose toxicity and stability concerns, Ba(Alo.5Nbo.5)O₃ is a lead-free, environmentally friendly perovskite with high thermal stability, making it a more suitable material for long-term outdoor solar applications. Additionally, its strong UV absorption capability makes it beneficial for tandem solar cells, where it can function as an effective wide-bandgap absorber layer, or as a UV-blocking layer in perovskite-silicon tandem solar cells, thereby improving the lifetime and efficiency of the underlying active layers.

Despite its potential, several challenges must be addressed to optimize Ba(Alo.sNbo.s)O₃ for practical solar cell applications. One of the key areas of improvement is bandgap tuning through elemental doping, where transition metal dopants such as Fe or Cu could allow for fine-tuning of the bandgap while enhancing charge carrier mobility. Additionally, thin-film deposition techniques must be developed to integrate Ba(Alo.sNbo.s)O₃ into solar cell architectures, ensuring uniform film formation for efficient charge transport and reduced recombination losses. Future work should also include detailed charge transport studies to measure carrier mobility, lifetime, and recombination dynamics. Furthermore, prototype solar cells using Ba(Alo.sNbo.s)O₃ as an absorber or charge transport layer should be fabricated and tested to evaluate its actual photovoltaic performance.

In conclusion, Ba(Alo.sNbo.s)O₃ presents a promising alternative to conventional perovskites due to its optimal bandgap, lead-free composition, and thermal stability. With further material optimization and device integration, this perovskite could contribute significantly to the development of next-generation solar cells with improved efficiency and longevity.

Volume 18, No. 4, 2024

ISSN: 1750-9548

V. Challenges & Future Work

Despite its potential, further studies are required to optimize Ba(Alo.sNbo.s)O3 for practical solar cell applications. One of the key areas of improvement is bandgap tuning via doping, where elemental doping with transition metals such as Fe or Cu could be explored to fine-tune the bandgap while enhancing charge carrier mobility. Doping can modify the electronic structure of the material, improving its absorption properties and optimizing its efficiency in photovoltaic applications. Another critical challenge is the thin-film deposition of Ba(Alo.sNbo.s)O3, which remains a major hurdle for device integration. The development of solution-based or vapor-phase deposition techniques could lead to improved thin-film uniformity, ensuring better contact with charge transport layers, enhancing charge collection, and minimizing recombination losses.

Additionally, testing charge carrier mobility and photovoltaic performance is essential for assessing the feasibility of Ba(Alo.sNbo.s)O₃ in real-world solar cell applications. Future studies should focus on measuring carrier mobility, lifetime, and recombination dynamics to understand the charge transport mechanisms within the material. Furthermore, fabricating prototype solar cells using Ba(Alo.sNbo.s)O₃ as an absorber or charge transport layer would provide experimental validation of its performance. These optimizations will be critical in establishing Ba(Alo.sNbo.s)O₃ as a viable candidate for next-generation lead-free, stable, and high-efficiency perovskite solar cells.

VI. CONCLUSION

In this study, Ba(Alo.5Nbo.5)O₃ perovskite was successfully synthesized using the solid-state reaction method, and its structural, morphological, optical, and surface properties were thoroughly investigated. X-ray diffraction (XRD) analysis confirmed the formation of a cubic perovskite phase, validating the material's crystallographic stability. Scanning Electron Microscopy (SEM) and Energy Dispersive X-ray Spectroscopy (EDS) revealed a uniform morphology with the correct elemental composition, confirming the successful incorporation of Ba, Al, and Nb into the perovskite structure. UV-Vis spectroscopy and Tauc plot analysis determined a direct bandgap of 1.56 eV and an indirect bandgap of 1.32 eV, which are well within the optimal range for single-junction solar cells, making this material a promising candidate for photovoltaic applications.

Despite these promising findings, further research is needed to optimize Ba(Alo.sNbo.s)O₃ for practical solar cell applications. Future work should focus on investigating thin-film deposition techniques, such as spray pyrolysis and pulsed laser deposition, to improve film quality and enhance charge transport properties. Additionally, bandgap engineering through doping strategies could be explored to fine-tune optical and electronic properties, optimizing the material for higher power conversion efficiency. Moreover, a detailed study of the electrical transport properties and carrier dynamics in solar devices is essential to evaluate charge mobility, recombination rates, and long-term stability under operating conditions. With these advancements, Ba(Alo.sNbo.s)O₃ has the potential to become a stable, lead-free alternative for next-generation high-performance perovskite solar cells.

REFERENCES

- [1] Fabian C. Hanusch, Erwin Wiesenmayer, Eric Mankel, Andreas Binek, Philipp Angloher, Christina Fraunhofer, Nadja Giesbrecht, Johann M. Feckl, Wolfram Jaegermann, Dirk Johrendt, Thomas Bein, Pablo Docampo, "Efficient Planar Heterojunction Perovskite Solar Cells Based on Formamidinium Lead Bromide," The Journal of Physical Chemistry Letters, 2014. (IF: 5)
- [2] Wan-Jian Yin, Ji-Hui Yang, Joongoo Kang, Yanfa Yan, Su-Huai Wei, "Halide Perovskite Materials for Solar Cells: A Theoretical Review," Journal of Materials Chemistry, 2015. (IF: 8)
- [3] Byung-Wook Park, Bertrand Philippe, Xiaoliang Zhang, Håkan Rensmo, Gerrit Boschloo, Erik M. J. Johansson, "Bismuth-Based Hybrid Perovskites A₃Bi₂I₉ (A: Methylammonium or Cesium) for Solar Cell Application," Advanced Materials, 2015. (IF: 8)
- [4] Mengjin Yang, Dong Hoe Kim, Talysa R. Klein, Zhen Li, Matthew O. Reese, Bertrand J. Tremolet de Villers, Joseph J. Berry, Maikel F.A.M. van Hest, Kai Zhu, "Highly Efficient Perovskite Solar Modules by Scalable Fabrication and Interconnection Optimization," ACS Energy Letters, 2018. (IF: 5)

- [5] M. Khalaji Assadi, Shokoufeh Bakhoda, Rahman Saidur, Hengameh Hanaei, "Recent Progress in Perovskite Solar Cells," Renewable & Sustainable Energy Reviews, 2018. (IF: 4)
- [6] Yang Wang, Peng Wang, Xue Zhou, C. Li, Huizeng Li, Xiaotian Hu, Fengyu Li, Xiaoping Liu, Mingzhu Li, Yanlin Song, "Diffraction-Grated Perovskite Induced Highly Efficient Solar Cells Through Nanophotonic Light Trapping," Advanced Energy Materials, 2018. (IF: 4)
- [7] Ajay Kumar Jena, Ashish Kulkarni, Tsutomu Miyasaka, "Halide Perovskite Photovoltaics: Background, Status, and Future Prospects," Chemical Reviews, 2019. (IF: 8)
- [8] K. B. Bhojanaa, A. S. Soundarya Mary, K. S. Shalini Devi, N. Pavithra, A. Pandikumar, "Account of Structural, Theoretical, and Photovoltaic Properties of ABO₃ Oxide Perovskites Photoanode-Based Dye-Sensitized Solar Cells," Solar RRL, 2021. (IF: 3)
- [9] Minhaj Ahmad, Abdurrahman Akib, M. Raihan, A. Shams, "ABO₃ Perovskites' Formability Prediction and Crystal Structure Classification Using Machine Learning," 2022 International Conference on Innovations in Science..., 2022.
- [10] Minhaj Uddin Ahmad, A. Abdur Rahman Akib, Md. Mohsin Sarker Raihan, Abdullah Bin Shams, "ABO₃ Perovskites' Formability Prediction and Crystal Structure Classification Using Machine Learning," arXiv-cond-mat.mtrl-sci. 2022.
- [11] M. N. Mattur, N. Nagappan, S. Rath, T. Thomas, "Prediction of Nature of Band Gap of Perovskite Oxides (ABO₃) Using a Machine Learning Approach," Journal of Materiomics, Elsevier, 2022.
- [12] N. Bibi, M. Usman, "A Theoretical Investigation of ABO₃ (A= Na and B= Ti, In) Perovskites for Solar Cell and Optoelectronic Applications," Materials Science in Semiconductor Processing, Elsevier, 2025.
- [13] N. Bibi, M. Usman, S. Noreen, "Predictions on New Cu-Based ABO₃ (A= Cu and B= Lu, Y) Oxide-Perovskite for Energy Storage and Optoelectronic Applications: A DFT Study," Materials Science in Semiconductor Processing, Elsevier, 2025.
- [14] V. A. Pandit, G. R. Repe, J. D. Bhamre, and N. D. Chaudhari, "A review on green synthesis and characterization technique for ferrite nanoparticles and their applications," in Journal of Physics: Conference Series, 2020. doi: 10.1088/1742-6596/1644/1/012009.
- [15] V. K. Kashte, N. N. Kapse, V. A. Pandit, and B. G. Toksha, "A Review on Graphene Oxide-Based Ferrite Nanocomposites for Catalytic Applications," 2024, Springer. doi: 10.1007/s10563-024-09434-1.
- [16] V. Ashok Pandit, N. N. Kapse, V. K. Kashte, and N. D. Chaudhari, "Magnetic Behaviour, and initial permeability of green synthesized Co2+ substituted Ni-Zn ferrite," J Magn Magn Mater, vol. 601, Jul. 2024, doi: 10.1016/j.jmmm.2024.172184.
- [17] Pandit, Vishal Ashok, et al. "Removal of methylene blue dye with cr3+ doped mg-zn ferrites prepared with the use of lemon juice." BIOINFOLET-A Quarterly Journal of Life Sciences 19.2 (2022): 181-185.
- [18] Pandit, Vishal Ashok, et al. "Properties of cr doped NI-ZN ferrite nanoparticles synthesized using lemon juice." BIOINFOLET-A Quarterly Journal of Life Sciences 19.2 (2022): 177-180.
- [19] Pandit, Vishal Ashok, et al. "Study on the green synthesis and characterization of Co2+ doped Mg–Zn ferrite nanoparticles using orange juice extract." Applied Physics A 130.12 (2024): 869.